

sides *Nucleotides* 8, 987-990.  
 Watling, D., Serafinowska, H. T., Reese, C. B., & Kerr, I. M. (1985) *EMBO J.* 4, 431-436.  
 Wells, V., & Mallucci, L. (1985) *Exp. Cell Res.* 159, 27-36.

Wreschner, D. H., James, T. C., Silverman, R. H., & Kerr, I. M. (1981) *Nucleic Acids Res.* 9, 1571-1578.  
 Wreschner, D. H., Silverman, R. H., James, T. C., Gilbert, C. S., & Kerr, I. M. (1982) *Eur. J. Biochem.* 124, 261-268.

## Differential Scanning Calorimetry of the Unfolding of Myosin Subfragment 1, Subfragment 2, and Heavy Meromyosin<sup>†</sup>

John W. Shriver\* and Utpala Kamath<sup>†</sup>

Department of Medical Biochemistry, School of Medicine, and Department of Chemistry and Biochemistry, Southern Illinois University, Carbondale, Illinois 62901

Received July 26, 1989; Revised Manuscript Received November 7, 1989

**ABSTRACT:** The thermal unfolding of rabbit skeletal heavy meromyosin (HMM), myosin subfragment 1, and subfragment 2 has been studied by differential scanning calorimetry (DSC). Two distinct endotherms are observed in the DSC scan of heavy meromyosin. The first endotherm, with a  $T_m$  of 41 °C at pH 7.9 in 0.1 M KCl, is assigned to the unfolding of the subfragment 2 domain of HMM based on scans of isolated subfragment 2. The unfolding of the subfragment 2 domain is reversible both in the isolated form and in HMM. The unfolding of subfragment 2 in HMM can be fit as a single two-state transition with a  $\Delta H_{vh}$  and  $\Delta H_{cal}$  of 161 kcal/mol, indicating that subfragment 2 exists as a single domain in HMM. The unfolding of subfragment 2 is characterized by an extraordinarily large  $\Delta C_p$  of approximately 30 000 cal/(deg·mol). In the presence of nucleotides, the high-temperature HMM endotherm with a  $T_m$  of 48 °C shifts to higher temperature, indicating that this peak corresponds to the unfolding of the subfragment 1 domain. This assignment has been confirmed by comparison with isolated subfragment 1. The stabilizing effect of AMPPNP was significantly greater than that of ADP. The vanadate-trapped ADP species was slightly more stable than M-AMPPNP with a  $T_m$  at 58 °C. The unfolding of subfragment 1, both in the isolated form and in HMM, was irreversible. Only a single endotherm was noted in the DSC scans of the subfragment 1 domain of HMM and in freshly prepared subfragment 1 complexes. There is no evidence in the DSC data for preferential stabilization of any subdomain of the head by the binding of nucleotides.

Scanning calorimetry provides an experimental demonstration of cooperative domain structure and domain interactions in proteins (Privalov, 1979; Sturtevant, 1987). The term "domain" has been used in various ways to describe structural units in a folded protein (Privalov, 1982; Zehfus, 1987; Vibert & Cohen, 1988). The most straightforward, objective, and experimentally testable definition of a domain is an independent, cooperative unit. A domain may affect the stability of neighboring domains, but their folded structure is independent. According to this definition, domains can be experimentally demonstrated by observing the unfolding reactions of proteins.

Protein unfolding can be followed by a number of techniques: e.g., by monitoring changes in circular dichroism, fluorescence, NMR spectra, and proteolytic rates. Analysis of proteolysis data can be complicated since the proteolysis itself may influence the unfolding process. Spectroscopic probes can be used to determine the equilibrium constant of the unfolding reaction as a function of temperature, from which an apparent van't Hoff enthalpy can be derived if the process is reversible (Privalov, 1979, 1982). Differential scanning calorimetry (DSC) provides not only an indication of the progress of the unfolding reaction (and therefore a van't

Hoff enthalpy) but also a direct measure of the enthalpy of the process (a calorimetric enthalpy) (Privalov, 1979). The calorimetric and van't Hoff enthalpies are equal for single-domain proteins (Privalov, 1979; Sturtevant, 1987). For proteins with multiple domains, either there will be multiple peaks in the DSC scan or, if the peaks overlap, the calorimetric enthalpy will exceed the van't Hoff enthalpy.

Myosin is an oligomeric protein of molecular weight 530 000 (Harrington & Rodgers, 1984). It is composed of two heavy chains and four light chains. The amino-terminal residues of the heavy chain fold to form a globular head, and the remainder of the molecule is involved in dimerization to form an extended coiled-coil segment. It is the globular heads which contain the ATPase and actin binding sites. The globular heads can be isolated in homogeneous form following limited proteolysis of myosin with  $\alpha$ -chymotrypsin in the presence of EDTA (Weeds & Taylor, 1975; Margossian & Lowey, 1982). The isolated heads are referred to as subfragment 1. Proteolysis of myosin with  $\alpha$ -chymotrypsin in the presence of excess divalent cations yields heavy meromyosin and light meromyosin (Weeds & Pope, 1977). Heavy meromyosin is a water-soluble two-headed fragment lacking a large part of the helical rod. The largely helical portion of heavy meromyosin (HMM)<sup>1</sup> linking the two heads together is referred to as subfragment 2, and may be obtained by treating HMM

<sup>†</sup> This work was supported by a research grant from the National Institutes of Health (AR37174). J.W.S. is the recipient of an NIH Research Career Development Award (AR01788).

\* Author to whom correspondence should be addressed at the Department of Chemistry and Biochemistry, Southern Illinois University.

<sup>†</sup> Present address: Department of Chemistry, University of California, Davis, CA.

<sup>1</sup> Abbreviations: DTE, dithioerythritol; S-1, myosin subfragment 1; S-2, myosin subfragment 2; HEPES, *N*-(2-hydroxyethyl)piperazine-*N'*-2-ethanesulfonic acid; HEPPS, *N*-(2-hydroxyethyl)piperazine-*N'*-3-propanesulfonic acid; HMM, heavy meromyosin;  $T_m$ , midpoint temperature of a transition; TRIS, tris(hydroxymethyl)aminomethane.

with  $\alpha$ -chymotrypsin in the presence of EDTA (Sutoh et al., 1978).

The domain nature of myosin has been of interest for a number of reasons. The subfragment 2 region is largely  $\alpha$ -helical and is believed to be a domain which can melt, or unfold, in a manner dictated by the form of the nucleotide in the active site on the globular head when myosin is organized into filaments (Harrington & Ueno, 1987). In addition, it has been shown that a wide variety of proteolytic enzymes are capable of producing three fragments of subfragment 1 with masses of 27, 50, and 20 kDa (Mornet et al., 1981, 1984). The three fragments remain associated following proteolysis, indicating that they may be formed as a result of nicking of exposed structureless loops. Many workers have referred to these fragments as domains, and recent evidence would seem to support this contention (Muhlrad & Morales, 1984; Chaussepied et al., 1986). Probably the most important is the claim that a stable active "S-1" which lacks the 20-kDa fragment can be prepared (Okamoto & Sekine, 1987). In addition, fragments of myosin have been isolated which possess ATP-dependent actin binding (Griffiths & Trayer, 1989). However, it is not clear if the boundaries of domains in the globular head actually coincide with the ends of the fragments, and it is probably not correct to speak of the fragments as domains. The observation that a portion of a fragment can fold into a structure resembling that found in the native protein does not imply that the fragment represents a domain.

Subfragment 2 has been proposed to be an important element in force production leading to muscle contraction (Harrington & Ueno, 1987). Evidence has been provided which demonstrates that a portion of the helical S-2 segment of myosin is unfolded following initiation of contraction. This helix-coil transition may play a role in providing contractile force. Recent evidence would seem to indicate that this model is incomplete (Hynes et al., 1987). DSC studies of subfragment 2 have been performed by a few laboratories (Swenson & Ritchie, 1980; Cross et al., 1984). No DSC studies have been reported of myosin fragments which include the ATPase active site.

Investigators of the enzymology of myosin have long been aware of the heat sensitivity of myosin and the irreversible nature of the unfolding, or denaturation, of myosin (Jacobson & Henderson, 1973). It has been shown that nucleotides, ATP in particular, are able to stabilize myosin and protect it against heat denaturation. Evidence has been presented for the differential thermal stability of a portion of the S-1 head (Burke et al., 1987; Cheung & Reisler, 1988).

#### MATERIALS AND METHODS

**Protein Preparations.** Myosin was prepared as described previously (Margossian & Lowey, 1982; Kamath & Shriver, 1989) from the back and leg muscle of a freshly sacrificed young adult White New Zealand rabbit. Heavy meromyosin was prepared by limited proteolysis using  $\alpha$ -chymotrypsin. A 2-min digestion of myosin was typically used to ensure retention of the LC2 light chain (Wagner, 1984; Kay et al., 1987). Long subfragment 2 was prepared from purified HMM with  $\alpha$ -chymotrypsin as described by Sutoh et al. (1978). S-1 was prepared with  $\alpha$ -chymotrypsin as described previously (Margossian & Lowey, 1982; Shriver & Sykes, 1981), or with trypsin as described by Balint et al. (1978).

The purity of all protein preparations was monitored by SDS gel electrophoresis (Figure 1). Gels were stained with Coomassie blue stain and scanned at 633 nm with an LKB Ultrascan XL enhanced laser densitometer interfaced to an IBM PS2 computer. The S-2 preparation typically showed a major

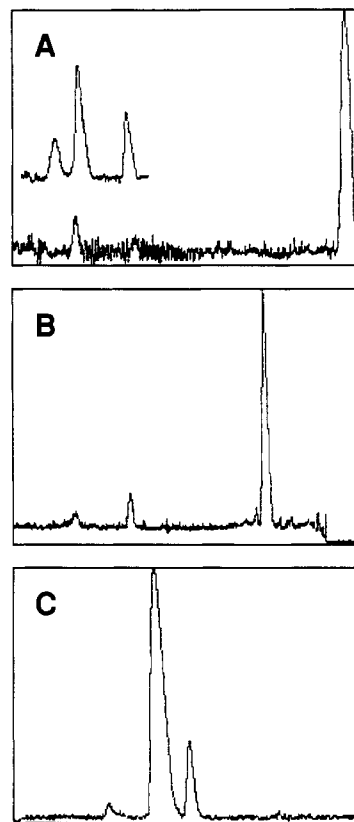


FIGURE 1: Densitometer scans of sodium dodecyl sulfate-acrylamide gels of heavy meromyosin, subfragment 1, and subfragment 2. The three gels were run at different times and are not aligned. The top of each gel is on the right. Panel A shows the heavy meromyosin heavy chain (140 kDa) and the three light chains with molecular weights of 21K, 19K, and 16.5K. The inset is the light-chain portion of a gel of the same sample run at higher loading. Panel B shows the subfragment 1 heavy chain with the two alkali light chains at 21 and 16.5 kDa. Panel C shows the subfragment 2 preparation with the major fraction (83%) at 60 000 Da. Two additional fragments appear at approximately 75 kDa (14%) and 50 kDa (3%). Molecular weight standards (phosphorylase *b*, bovine serum albumin, ovalbumin, and carbonic anhydrase) were run simultaneously with the S-2 (data not shown).

band at 60 000 daltons on SDS gels with minor bands at 74 000 and 50 000 daltons, as demonstrated by Sutoh et al. (1978).  $K^+$ -EDTA ATPase activities of HMM and S-1 were monitored as previously described using a Radiometer pH stat (Shriver & Sykes, 1981). Heavy meromyosin, subfragment 1, and subfragment 2 protein concentrations were determined by UV absorbance at 278 nm on a Cary 210 spectrophotometer using the following published extinction coefficients:  $\epsilon_{278\text{nm}}^{1\%} = 7.5, 6.0, \text{ and } 0.7 (\times 10^2 \text{ cm}^2/\text{g})$  for S-1, HMM, and S-2, respectively (Margossian & Lowey, 1982). Due to its importance in this work, the S-2 concentration was also determined by using the biuret assay with crystalline bovine serum albumin as a standard. The results of the two measurements of the S-2 concentration agreed to within 10–15%. The absorbance accuracy of the Cary 210 instrument was determined with an alkaline potassium chromate solution (Gordon & Ford, 1972).

Sodium orthovanadate was purchased from Alfa. A 5 mM solution in 50 mM TRIS (pH 7.9), 0.1 M KCl, and 1 mM  $\text{MgCl}_2$  was heated to 100 °C in a boiling water bath for 10 min prior to use (Goodno, 1979).

**Differential Scanning Calorimetry.** Scanning calorimetry experiments were performed in TRIS, HEPES, HEPPS, and phosphate buffers. The pH of all buffers was adjusted at 25 °C.  $\text{MgCl}_2$  was present in all experiments reported here to

allow nucleotide binding, or to permit comparison with such experiments. A high pH (i.e., 7.9–8.0) was chosen to minimize aggregation (Ueno et al., 1983). We have obtained the best DSC base lines with HMM in TRIS buffer, and some experiments have been performed in HEPES and phosphate buffers. The enthalpies determined here are much larger than the heat expected to be involved in proton neutralization. Goodno and Swenson (1975) have estimated that two protons are absorbed at pH 6.5 under myosin unfolding.

Differential scanning calorimetry was performed with a Microcal MC2 scanning calorimeter. Protein solutions were exhaustively dialyzed against the indicated buffer overnight. The sample cell was loaded with 1.229 mL of solution. The final buffer which the protein had been dialyzed against was used to fill the reference cell. The cells were operated under approximately 30 psi of nitrogen during each scan. In most experiments, DSC scans were performed at a relatively rapid rate of 90 °C/h to minimize aggregation problems. Samples were not degassed. Instead, typically the sample was preheated 3 times in the DSC instrument by scanning to 35 °C (i.e., below any denaturation endotherm), followed by rapid cooling. This procedure resulted in the flattest and most reproducible instrumental base lines.

All DSC experiments were under computer control using an IBM PC computer interfaced to the Microcal MC2 instrument. The computer interface and data collection software were supplied by Microcal. Multiple, repetitive scans were performed on the same sample to check for reversibility, with identical cooling and equilibration times between scans.

**DSC Data Analysis.** The DSC raw data, in the form of heat flow (millicalories per minute) as a function of temperature, were transferred from the IBM PC to a Macintosh II computer using MacLinkPlus (Data Viz, Inc., Norwalk, CT). The raw data were then converted to excess heat capacity (kilocalories per degrees centigrade per mole) by dividing each data point by the scan rate and the number of moles of protein in the sample cell.

The DSC heat capacity data were fit by using nonlinear least-squares fitting routines on a Macintosh II computer. The data were initially fit by assuming that  $\Delta H_{\text{cal}}/\Delta H_{\text{vh}} = 1$ . If the resulting fit was not satisfactory, the  $\Delta C_p$  was removed from the data as described below, and the data were fit by allowing  $\Delta H_{\text{cal}}$  and  $\Delta H_{\text{vh}}$  to float. The programs were written to supply the midpoint temperature of the transition, the calorimetric and van't Hoff enthalpies of the transition, and the  $\Delta C_p$  of the transition. Test data were analyzed with these programs and also the software supplied with the Microcal MC2 instrument (source code not available) to determine if any errors or bugs existed in the programs used here. The basis of the programs is briefly outlined below, and a source code listing of the programs is available from one of the authors (J. Shriver).

**(A) Program 1. Two-State Unfolding Transition ( $\Delta H_{\text{cal}} = \Delta H_{\text{vh}}$ ) with a Nonzero  $\Delta C_p$ .** The equilibrium constant for an unfolding reaction at any temperature  $T$  is given by

$$K(T) = \exp[-\Delta G(T)/RT] \quad (1)$$

where  $R$  is the gas constant,  $T$  is the temperature in degrees kelvin, and the Gibbs free energy change,  $\Delta G$ , at temperature  $T$  is given by

$$\Delta G(T) =$$

$$\Delta H(T_m) + \int_{T_m}^T \Delta C_p dT - T\Delta S(T_m) - T \int_{T_m}^T (\Delta C_p/T) dT \quad (2)$$

or

$$\Delta G(T) =$$

$$\Delta H(T_m) \left( \frac{T_m - T}{T_m} \right) - (T_m - T)\Delta C_p + T\Delta C_p \ln \left( \frac{T_m}{T} \right) \quad (3)$$

where  $T_m$  is the midpoint of the transition when  $K = 1$  (Privalov et al., 1986). Knowing  $K$  at any temperature, the progress  $\alpha(T)$  of the reaction at temperature  $T$  is given by

$$\alpha(T) = \frac{K(T)}{1 + K(T)} \quad (4)$$

Upon substitution of eq 1 and 3 into eq 4, the progress of the reaction at any temperature  $T$  can be expressed as a function of  $T$ ,  $\Delta H(T_m)$ ,  $T_m$ , and  $\Delta C_p$ . The excess heat capacity in a DSC scan is then given by the temperature dependence of the reaction progress multiplied by the enthalpy change for the reaction at that temperature (Sturtevant, 1987)

$$c_{\text{excess}} = \Delta H(T) \frac{d\alpha(T)}{dT} \quad (5)$$

where we allow  $\Delta H$  to be temperature dependent:

$$\Delta H(T) = \Delta H(T_m) + \int_{T_m}^T \Delta C_p dT \quad (6)$$

$$\Delta H(T) = \Delta H(T_m) + (T - T_m)\Delta C_p \quad (7)$$

Following Sturtevant (1987), the base line for a DSC scan is given by a weighted sum of two straight lines:

$$c_{\text{base line}} = [1 - \alpha(T)](A + BT) + \alpha(T)(C + DT) \quad (8)$$

The total excess heat capacity is  $c_{\text{total}} = c_{\text{excess}} + c_{\text{base line}}$ . In practice, the DSC data are adjusted by a separate program prior to fitting so that the heat capacity and the slope of the base line prior to the transition are zero; i.e., both  $A$  and  $B = 0$ . If  $T$  is expressed relative to the midpoint temperature,  $T_m$ , then  $C$  is  $\Delta C_p$  at  $T_m$  and

$$c_{\text{base line}} = \alpha(T)[\Delta C_p + D(T - T_m)] \quad (9)$$

The total excess heat capacity is now defined by four parameters [i.e.,  $T_m$ ,  $\Delta H(T_m)$ ,  $\Delta C_p$ , and  $D$ ], and the data are fit to the expression for  $c_{\text{total}}$  by using a four-parameter nonlinear least-squares fitting program.

**(B) Program 2. Non-Two-State Unfolding Transition with  $\Delta H_{\text{cat}} > \Delta H_{\text{vh}}$ .** The simultaneous unfolding of multiple independent domains with similar midpoint temperatures, such that only one endotherm is observed, results in the observed  $\Delta H_{\text{cal}}$  being greater than  $\Delta H_{\text{vh}}$ . A simple example might be the overlapping of two two-state transitions with identical  $\Delta H_{\text{cal}}$ 's, and as a result, the area of the endotherm (i.e., the total observed  $\Delta H_{\text{cal}}$ ) would be twice that expected from the width of the transition. If

$$\beta = \Delta H_{\text{cal}}/\Delta H_{\text{vh}} \quad (10)$$

then

$$c_{\text{excess}} = \beta \Delta H(T) \frac{d\alpha(T)}{dT} \quad (11)$$

However, a problem arises in fitting such data since, in the

<sup>2</sup> Standard-state free energies, enthalpies, entropies, and heat capacities are implied throughout in all the equations. Since there is no change in mole number in the unfolding reactions and the activity coefficients are assumed to be 1 throughout the DSC scans, non standard- and standard-state quantities are identical.

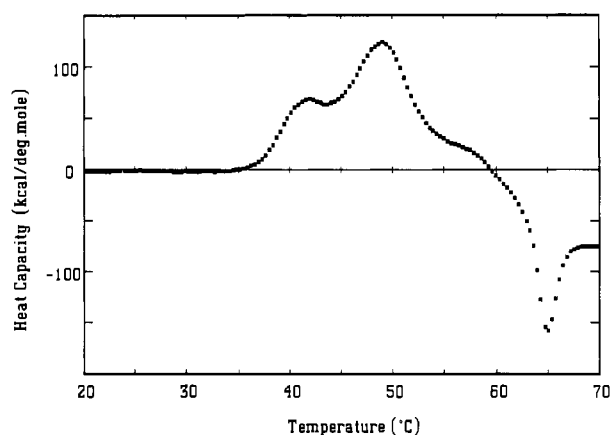


FIGURE 2: DSC scan of heavy meromyosin at pH 7.9. The protein was dialyzed extensively against 50 mM TRIS (pH 7.9), 0.1 M KCl, 1 mM  $\text{MgCl}_2$ , and 1 mM DTE. The HMM concentration was 12  $\mu\text{M}$ . The scan rate was 90  $^{\circ}\text{C}/\text{h}$ , and data were collected every 15 s.

absence of assuming a particular model, we do not know the magnitudes of  $\Delta C_p$  for each independent transition. The observed  $\Delta C_p$  is the sum of the  $\Delta C_p$ 's for each independent two-state transition. The relative magnitudes of the individual  $\Delta C_p$ 's are not defined by the DSC scan, and it is not possible to use the complete expression for  $\Delta G$  (eq 2) in fitting the data. Therefore, if there is a  $\Delta C_p$ , it must be removed prior to doing a fit as follows. A reflection of the progress of the reaction at any temperature  $T$  is obtained by calculating a progress function,  $I(T)$ , by taking the ratio of the integral of the DSC scan from any arbitrary temperature,  $T_i$ , preceding the transition up to any temperature  $T$ , divided by the total integral over the transition. In practice, a summation of the excess heat capacity data is used instead of an integration:

$$I(T) = \frac{\sum_{t=T_i}^T C_p(t)}{\sum_{t=T_i}^{T_f} C_p(t)} \quad (12)$$

Such a function is linear before and after the transition, and a smooth sigmoidal transition from one linear section to the

other occurs in the temperature range of the reaction. An equilibrium constant is obtained from the progress curve at any temperature  $T$  in the usual manner (a two-state reaction can be assumed for this purpose without introducing significant error), and  $\alpha(T)$  is calculated by using eq 3, and  $c_{\text{base line}}$  is calculated at temperature  $T$  by using values for  $A$ ,  $B$ ,  $C$ , and  $D$  obtained from fitting segments of the base line before and after the transition in the DSC scan. In practice,  $c_{\text{base line}}$  occasionally contains a singularity, so  $c_{\text{base line}}$  is smoothed by fitting with a nonlinear least-squares fitting program. The fitted  $c_{\text{base line}}$  curve is subtracted from the original data, and the result is then fit to obtain  $\Delta H_{\text{cal}}$ ,  $\Delta H_{\text{vh}}$ , and  $T_m$ .

## RESULTS

Figure 2 shows the DSC scan obtained for heavy meromyosin at pH 7.9 in 0.1 M KCl with no nucleotide. Two prominent endotherms are seen: a shoulder with a  $T_m$  at 41  $^{\circ}\text{C}$  and a larger peak at 48  $^{\circ}\text{C}$ . The two endothermic peaks clearly indicate at least two domains. An exothermic process, leading to a negative peak, can be seen at approximately 65  $^{\circ}\text{C}$ . The position and magnitude of the exothermic peak were variable, and it is attributed to aggregation and precipitation of the unfolded protein. The unfolding of the second domain was irreversible. Exothermic peaks have been described for other irreversible protein unfolding reactions (Takahashi et al., 1981). The fastest scan rate available on the MC2 instrument was used to separate the exotherm from the endothermic transitions, since aggregation would be expected to be slower than unfolding. However, the irreversible step was quite fast since we were unable to partially unfold the sample by heating to the midpoint of the second transition.

In an effort to assign the two endotherms observed in Figure 2 to specific domains in HMM, we have studied the effects of nucleotide binding on the DSC scan. Figure 3 shows the effect of adding excess ADP, AMPPNP, and ADP with vanadate. The addition of ADP alone slightly shifted the higher temperature endotherm to higher temperature by 2  $^{\circ}\text{C}$ , whereas AMPPNP and ADP-V had a more significant stabilizing effect on the domain corresponding to the high-tem-

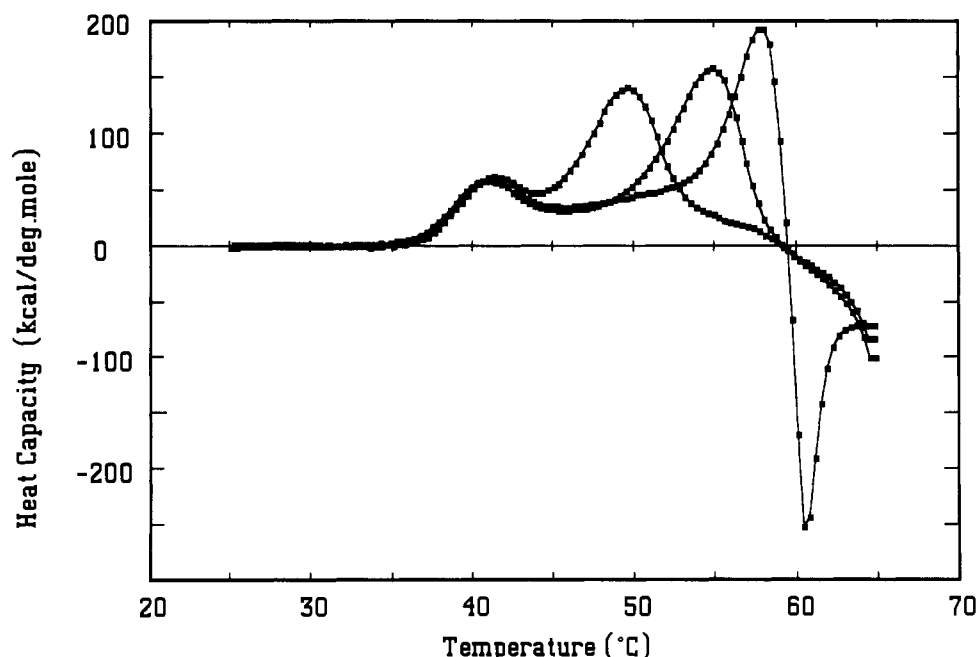


FIGURE 3: DSC scans of heavy meromyosin in the presence of nucleotides. The high-temperature endotherm of HMM was increasingly shifted to higher temperature by binding ADP, AMPPNP, and ADP-vanadate. Nucleotide had no noticeable effect on the  $T_m$  of the endotherm at 41  $^{\circ}\text{C}$ . Buffer conditions and protein concentration were as in Figure 2. The nucleotide concentration was 1 mM, and the vanadate concentration was 50  $\mu\text{M}$ .

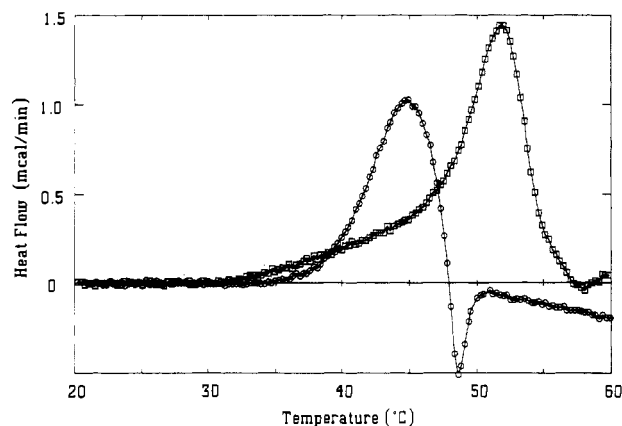


FIGURE 4: DSC scans for myosin subfragment 1. The conditions were 50 mM TRIS, 0.6 M KCl, 5 mM  $\text{MgCl}_2$ , and 1 mM DTE at pH 8.0. The concentration of S-1 was 13.8  $\mu\text{M}$ , and the scan rate was 60  $^\circ\text{C}/\text{h}$ . The leftmost scan, shown with open circles with a maximum at approximately 45  $^\circ\text{C}$ , was obtained in the absence of nucleotide. The rightmost scan, shown with open squares with a maximum at 52  $^\circ\text{C}$ , was obtained in the presence of 0.88 mM AMPPNP.

perature endotherm, viz., 7 and 10  $^\circ\text{C}$ , respectively. The most obvious conclusion from the data in Figure 3 is that only one of the two prominent endotherms is perturbed by the binding of nucleotide and this peak is assigned to the unfolding of the globular heads, or the S-1 domain. The peak at 41  $^\circ\text{C}$  is not affected by nucleotide binding, and this is assigned to the unfolding of the S-2 coiled-coil domain. This assignment is confirmed by studies with isolated S-1 and S-2 fragments.

The thermal unfolding of subfragment 1 prepared with  $\alpha$ -chymotrypsin is shown in Figure 4. Just as with the globular heads of HMM, the unfolding of S-1 was irreversible, and we commonly observed an aggregation exotherm with S-1. However, the problems with the exotherm were more severe than with HMM, since it almost always began prior to completion of the unfolding reaction. The magnitude and position of the exotherm varied with each experiment; however, the exotherm almost always overlapped the endotherm, making even a determination of the  $T_m$  difficult. In a few instances, we were able to scan through the  $T_m$  before the exothermic process began. The experiments shown in Figure 4 are our best results with subfragment 1 and were obtained under slightly different conditions than those used in the experiments presented in Figures 2 and 3. The irreversibility of the transition and the overlapping of a variable exothermic peak and an endothermic peak make a quantitative analysis of the S-1 data unreliable. The midpoint of the melting of S-1 under these conditions was at roughly 45  $^\circ\text{C}$ , and the calorimetric enthalpy of unfolding of S-1 was approximately 300 kcal/mol. The apparent van't Hoff enthalpy was 120 kcal/mol. The validity of both enthalpies is questionable. This is especially true of the  $\Delta H_{\text{vh}}$  due to the irreversibility of the unfolding. It is given here essentially as a phenomenological parameter describing the width of the observed transition. The binding of AMPPNP shifted the S-1 peak by approximately 7  $^\circ\text{C}$  to 52  $^\circ\text{C}$ . The slow rise in the excess enthalpy on the low-temperature side of the endothermic peak in both DSC scans is attributed to the irreversibility of the reaction. It may also reflect the dissociation and unfolding of the light chains. We have been unable to detect any pronounced endothermic peak in DSC scans of isolated light chains (M. Sabat, N. Khan, and J. Shriver, unpublished results). Significantly, the binding of AMPPNP resulted in the shifting of the entire endotherm and did not preferentially stabilize any particular domain in the S-1 structure. The increase in amplitude of the endotherm

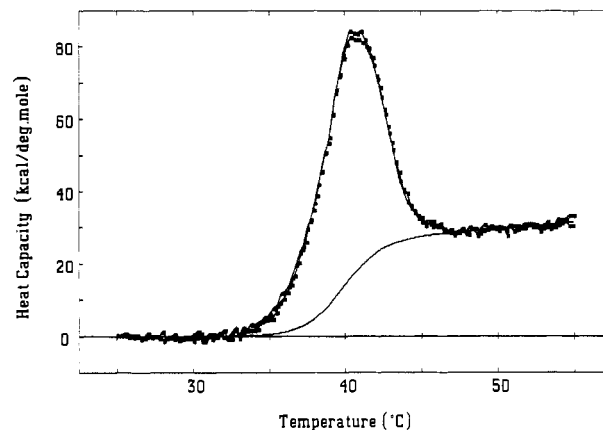


FIGURE 5: Two DSC scans for isolated long subfragment 2 at pH 7.9. The buffer was the same as in Figure 2, and the protein concentration was 9  $\mu\text{M}$ . Two consecutive scans on the same sample are shown to demonstrate the reversibility of the unfolding reaction. The sigmoidal base line, or reaction progress curve, was obtained by integration of the DSC data as described under Materials and Methods. The  $\Delta C_p$  obtained from the base line was 26 700 cal/(deg.mol) at the  $T_m$ .

upon binding AMPPNP is attributed to a positive  $\Delta C_p$  for unfolding.

The assignment of the endotherm in the DSC scan of HMM at 41  $^\circ\text{C}$  to the unfolding of the S-2 segment can be made based on the results of Swenson and Ritchie (1980). In order to confirm this, we prepared long S-2 from heavy meromyosin. The DSC results are shown in Figure 5. Only a single endotherm is observed at approximately 41  $^\circ\text{C}$ , which coincides with the first endotherm in the DSC scan of heavy meromyosin. The unfolding of isolated long S-2 is remarkably reversible, as indicated by the virtual overlap of two consecutive scans on the same sample in Figure 5.

The reversibility of the unfolding of isolated long S-2 led us to investigate the reversibility of the unfolding of the S-2 domain in HMM. The AMPPNP was used to shift the S-1 endotherm so that the unfolding of S-2 alone could be studied. The first scan (data not shown) was terminated at 45  $^\circ\text{C}$ , and the sample was cooled to approximately 10  $^\circ\text{C}$ . The time that the protein was held at a temperature between 35 and 45  $^\circ\text{C}$ , i.e., within a temperature range where significant unfolding of S-2 occurs, was approximately 15 min. Upon reheating, the second scan was observed to be essentially identical with the first, satisfying the criterion of reversibility. The unfolding of the S-1 domain was totally irreversible. We were unable to observe any endotherm in a second scan, even if the first scan only went halfway through the endotherm. In addition, the unfolding of the S-1 domain in HMM prevented the refolding of the S-2 domain upon cooling.

It is clear from the data in Figure 3 that we have an opportunity to analyze the DSC data without having to use deconvolution methods; i.e., we can use nucleotide binding to move the upper endothermic process out of the way to reveal the posttransition base line. Once the base line is defined on both sides of the transition, a reliable analysis of the DSC scan can be performed since the S-2 transition is reversible. Figure 6 shows the fitting of the S-2 endotherm of HMM assuming a two-state transition with a  $\Delta C_p$ , i.e., using the first program described under Materials and Methods. The fit results in a  $T_m$  of 39.8  $^\circ\text{C}$ , a  $\Delta H_{\text{vh}}$  of 161 kcal/(deg.mol), and a  $\Delta C_p$  of 30 200 cal/(deg.mol). The data were truncated to include only the main transition since a large  $\Delta C_p$  leads to a cold denaturation peak very close to the observed heat denaturation endotherm (note the upturn of the fitted excess heat capacity

Table I: Thermodynamic Parameters Derived from the DSC Data on Myosin Fragments

protein	pH	buffer	$T_m$ (°C)	$\Delta C_p$ [cal/(deg·mol)]	$\Delta H_{vh}$ (kcal/mol)	$\Delta H_{cal}$ (kcal/mol)
HMM						
S-1 domain with ADP	7.9	TRIS	49	<i>e</i>	172	518 <sup>a</sup>
S-2 domain with ADP·V	7.9	TRIS	39.8	30 200	161	161 <sup>b</sup>
with ADP·V	7.9	HEPES	41.8	31 100	171	171 <sup>b</sup>
S-1	7.9	TRIS	45	<i>e</i>	120	300 <sup>c</sup>
S-2	7.9	TRIS	40.3	26 700	150	351 <sup>d</sup>
	7.9	HEPES	39.8	27 200	147	399 <sup>d</sup>
	8.0	phosphate	39.9	29 600	155	435 <sup>d</sup>

<sup>a</sup> Fit by deconvolution of the two peaks in HMM-ADP. This is an irreversible transition, and the numbers are given primarily to describe the intensity and width of the endotherm. <sup>b</sup> Two-state transition assumed. <sup>c</sup> Irreversible transition. <sup>d</sup> Fit by removing  $\Delta C_p$  prior to fit. <sup>e</sup> Not determined.

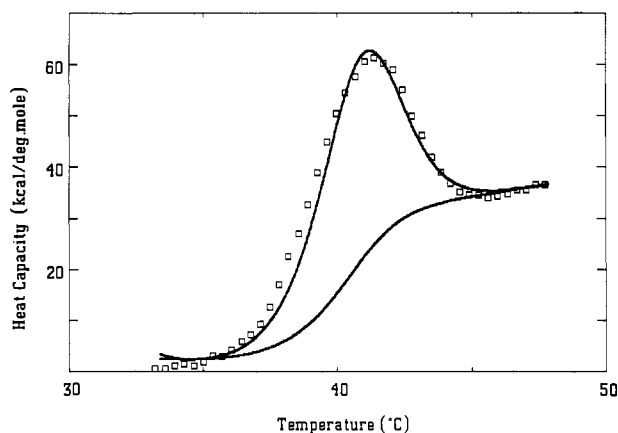


FIGURE 6: Fitting of the DSC data for the unfolding of the subfragment 2 domain of heavy meromyosin in the presence of ADP and vanadate. The data shown with open squares are a truncated portion of the data shown in Figure 3. The data were fit by assuming a two-state transition and allowing a simultaneous fitting of  $T_m$ ,  $\Delta C_p$ ,  $\Delta H$  (i.e.,  $\Delta H_{cal} = \Delta H_{vh}$ ), and the slope of the posttransition base line. The data were adjusted so that the  $y$  intercept and slope of the pretransition base line were zero. A slight upturn in the fitted heat capacity curve is seen at 33 °C and indicates the forcing of cold denaturation into the fit (by the large  $\Delta C_p$ ) since a temperature dependence in the  $\Delta C_p$  was not included in the fit. The resulting  $\Delta C_p$  was 30 253 cal/(deg·mol) with a  $\Delta H$  of 161 kcal/mol and a  $T_m$  of 39.8 °C.

curve at low temperature). We have not detected any indication of cold denaturation for the S-2 domain in scans down to 1 °C. Therefore,  $\Delta C_p$  must be temperature dependent. We do not have sufficient data to define the temperature dependence of  $\Delta C_p$ , so we have chosen to fit a truncated version of the data and assume no temperature dependence to  $\Delta C_p$ .

An alternative method of fitting the unfolding data for S-2 in HMM is to remove the progress curve of the reaction as described under Materials and Methods and then fit the data without requiring a  $\Delta C_p$  fit. The original data and the progress curve (obtained as described under Materials and Methods) are shown in Figure 7A. The  $\Delta C_p$  obtained from the progress curve is 26 500 cal/(deg·mol), and the excess heat capacity data after removal of the progress curve is shown in Figure 7B as open squares. Two fits were performed on the excess heat capacity data. The first assumed that the unfolding transition is not a two-state reaction, and results in a  $T_m$  of 40.6 °C, a  $\Delta H_{cal}$  of 185 kcal/mol, and a  $\Delta H_{vh}$  of 169 kcal/mol ( $\Delta H_{cal}/\Delta H_{vh} = 1.09$ ). This is the outer smooth curve through the data in Figure 7B. The second fit was done by assuming a two-state transition and gave a  $T_m$  of 40.6 °C and a  $\Delta H$  of 178 kcal/mol. There is little difference between the quality of the two fits, and it can be concluded that the unfolding of the S-2 domain of HMM occurs as a two-state transition. A similar analysis was performed with data collected on HMM in HEPES buffer (see Table I).

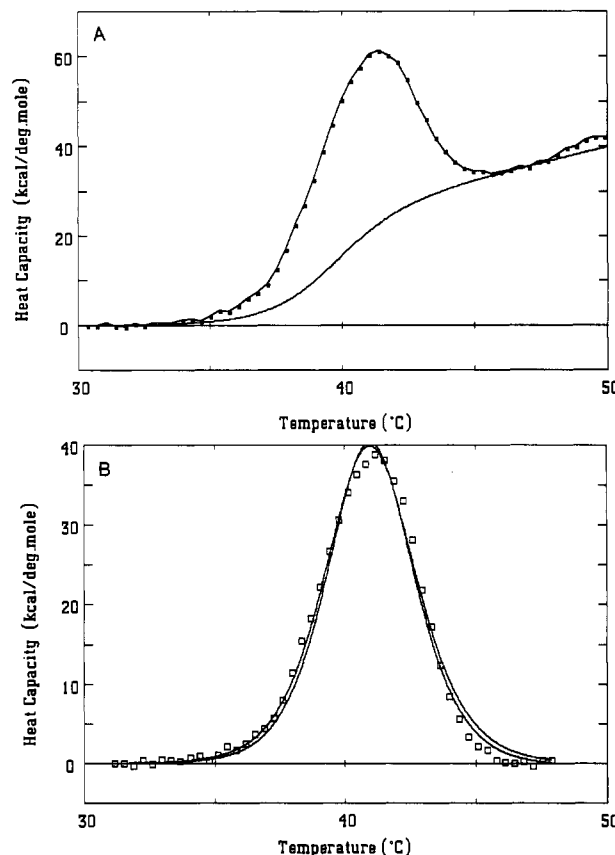


FIGURE 7: Alternative fitting of the unfolding of subfragment 2 domain in heavy meromyosin. In (A) is shown a truncated portion of the data shown in Figure 3 for HMM in the presence of ADP and V. The data points are simply connected to indicate the form of the DSC scan. The sigmoidal base line was obtained by integration of the DSC curve as described under Materials and Methods. (B) The excess heat capacity data [after removal of the sigmoidal base line shown in (A)] are shown with open squares. Two different fits of the data are shown with smooth solid curves through the data. The outer curve corresponds to a fit where  $\Delta H_{cal} \neq \Delta H_{vh}$  ( $\Delta H_{cal} = 185$  kcal/mol,  $\Delta H_{vh} = 169$  kcal/mol, and  $T_m = 40.6$  °C). The inner curve corresponds to a forced two-state fit ( $\Delta H_{cal} = \Delta H_{vh} = 178$  kcal/mol and  $T_m = 40.6$  °C).

In contrast, the DSC data for isolated S-2 (Figure 5) could not be adequately fit as a two-state transition. Therefore, the progress curve was removed as described under Materials and Methods. The total  $\Delta C_p$  for the transition was 26 700 cal/(deg·mol), and the excess heat capacity data are shown in Figure 8. The smooth curve through the data is the fit obtained by not requiring  $\Delta H_{cal} = \Delta H_{vh}$ . The calorimetric enthalpy of unfolding for long S-2 in TRIS buffer at pH 7.9 was calculated to be 350 kcal/mol, and the van't Hoff enthalpy was 150 kcal/mol with a  $T_m$  of 40.3 °C. A similar analysis of data collected in HEPES buffer at pH 7.9 was also per-

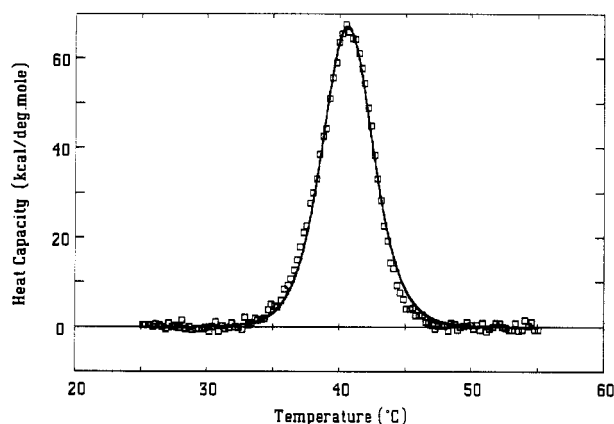


FIGURE 8: Fitting of the DSC data for isolated subfragment 2. The data from Figure 5 are shown (with open squares) after removal of the sigmoidal base line. The fit is shown by the smooth solid curve and corresponds to a  $\Delta H_{cal}$  of 351 kcal/mol and a  $\Delta H_{vh}$  of 150 kcal/mol with a  $T_m$  of 40.3 °C.

formed.  $\Delta H_{cal}$  was 399 kcal/mol, and  $\Delta H_{vh}$  was 147 kcal/mol with a  $T_m$  of 39.8 °C. The total  $\Delta C_p$  for the transition was 27 300 cal/(deg.mol).

Tryptic S-1 was prepared by treating chymotryptic S-1 with trypsin for 10 min (Balint et al., 1978). This resulted in the complete conversion of the 95-kDa band on SDS gels to 25-, 50-, and 20-kDa bands. The DSC scan indicated that there is negligible effect on the stability of the S-1 as a result of this treatment (data not shown). The midpoint of the unfolding endotherm is at 47 °C, and no new endotherms appeared as a result of trypsin digestion.

## DISCUSSION

We have initiated studies of the unfolding of myosin fragments, with an emphasis on those domains believed to be potentially involved in force production in muscle contraction. The goal is to provide a firm thermodynamic basis both for the existence of domains and for the interactions between domains, within the myosin molecule.

On the basis of DSC results with S-1 and S-2, the endotherm at approximately 41 °C in the DSC scan of HMM can be assigned to the melting of the S-2 domain, and the endotherm which occurs at higher temperature, and which is sensitive to nucleotide binding, can be assigned to the unfolding of the globular heads. The data presented here indicate that in the soluble form at physiological ionic strength there is no interaction between the subfragment 2 domain and the ATPase active site. By using AMPPNP, ADP-V, and ADP, we have chosen nucleotides which are believed to induce structural states in S-1 which are similar to those which exist during ATP hydrolysis. The thermal stability of the S-2 domain in HMM is unaffected by the binding of any of these nucleotides. It would therefore appear that there is no communication between the globular head and the S-2 segment of myosin at any stage of the ATP hydrolysis reaction. Of course in the filament there may be interactions present such that the nucleotide in the active site of one molecule may modulate the stability of the S-2 in a neighboring molecule. Interactions between the S-1 region of myosin and the S-2 region of a neighboring molecule in the filament are an essential element of the Harrington model for force production. The results presented here do not preclude this possibility.

However, the results presented here indicate that the domain structure of S-2 in HMM is different from that seen in isolated S-2. The van't Hoff and calorimetric enthalpies for the unfolding of the S-2 domain in HMM are equal, which clearly

indicates that S-2 is a single domain in HMM. In contrast, in isolated long S-2, the enthalpies are not equal, with the calorimetric enthalpy being roughly twice the van't Hoff enthalpy. This indicates that the unfolding of long S-2 occurs in more than one step, possibly indicating more than one domain. Swenson and Ritchie (1980) previously showed that a broad transition could be observed in the DSC scan of long S-2 at a lower temperature than the main endotherm in the region of pH 7. We have observed this transition also. Swenson and Ritchie assigned this endotherm to the hinge region in S-2 that Harrington proposed to be involved in force production in muscle contraction. As the pH was increased, this endotherm decreased in intensity and shifted to higher temperature. Under the conditions used here, this transition is most likely significantly broadened and lies under the major endotherm or at a higher temperature. Even in the region of pH 7.0 where this transition is obvious, its intensity is only a small fraction of the major endotherm. Therefore, this transition is not responsible for the large difference in  $\Delta H_{cal}$  and  $\Delta H_{vh}$  which we have observed for long S-2.

The results of the DSC analysis presented here for isolated long S-2 differ significantly from those of Sutoh et al. (1978). The DSC at pH 7.9 shows a single endotherm which cannot be fit as a single transition. In contrast, Sutoh et al. have studied the unfolding of long S-2 with optical rotatory dispersion (ORD) at pH 8.0 and observed that the unfolding transition is quite broad, beginning at approximately 20 °C and essentially finishing at 60 °C. They assumed a single two-state transition, and the van't Hoff enthalpy determined for this broad transition was 35 kcal/mol. However, there is difficulty in deciding what the base line should be for the  $[m]_{232}$  (mean residue rotation) data before and after the transition. Hvidt et al. (1985) have shown that there is an intrinsic temperature dependence in  $[m]_{232}$  for both  $\alpha$ -helices and random-coil model systems. If the data between 5 and 35 °C are assumed to define a pretransition base line, then most of the change in S-2 structure indicated by the ORD data occur between 40 and 50 °C, which would imply a  $\Delta H$  of roughly 150 kcal/mol.

It is interesting to note that Sutoh et al. (1978) observed a  $T_m$  of 45 °C in 0.1 M NaCl from the ORD data with no pH dependence between pH 6.2 and 8.0. In contrast, Swenson and Ritchie (1980) observed the  $T_m$  obtained from DSC scans to shift from 52 °C at pH 5.8 to 46 °C at pH 7.2 and 0.1 M KCl. While we have not performed a detailed pH and salt dependence study on S-2, what experiments that we have done at lower pH support the results of Swenson and Ritchie.

There are a number of explanations which might be put forth for the large difference in  $\Delta H_{cal}$  and  $\Delta H_{vh}$  observed for the unfolding of isolated long S-2. First, the most trivial is that the concentration of S-2 used to calculate  $\Delta H_{cal}$  could be incorrect. However, the concentration measured by using the published extinction coefficients agrees to within 10–15% with the value obtained by using the biuret assay. Second, S-2 preparations typically contain a small amount of a 74 000-Da fragment. Since the S-2 is made from purified HMM, the 74 000-Da fragment must be a long S-2 with a 14-kDa portion of the S-1 head attached. This would not be expected to double the  $\Delta H_{cal}$ . A rough calculation would indicate that the additional enthalpic contribution of this 14-kDa extension would be approximately 6 kcal/mol (i.e., 14 kDa/95 kDa times 300 kcal/mol times 13% contribution) which is well within the experimental error of the measurements. Third, the molecular weight of the cooperative unit of S-2 might be wrong; i.e., the two chains of the coiled-coil might separate in an S-2 prepa-



ration. However, the molecular weight of long S-2 has been determined to be 101 000 by sedimentation equilibrium (Sutoh et al., 1978). In addition, separated extended S-2 helices would not be expected to exist in solution.

It would therefore appear that isolated S-2 is composed of more than one significant domain. We need to ask why there is such a large difference between the results obtained for isolated S-2 and the S-2 domain in HMM. The large increase in  $\Delta H_{\text{cal}}$  observed for S-2 unfolding in going from HMM to isolated S-2 may be due to an altered structure in S-2 due to proteolysis. However, we would expect that such an effect would lead to loss of structure and a decrease in  $\Delta H_{\text{cal}}$ . It may be that in HMM a portion of S-2 is actually stabilized by the S-1 and does not unfold until S-1 unfolds.

It should be noted that the thermal stability of S-2 is not significantly different from that of a large portion of LMM (King & Lehrer, 1989; Shriver and Zegar, unpublished results). The  $T_m$  for S-2 is 41 °C compared to 43 °C for the first transition in LMM which comprises more than half of the total enthalpy involved in the unfolding of LMM.

The large  $\Delta C_p$  observed for the unfolding of both isolated S-2 and the S-2 domain of HMM is remarkable, viz., approximately 30 000 cal/(deg·mol) or 0.3 cal/(deg·g). Specific heat capacities of globular protein unfolding are typically in the range of 0.1–0.15 cal/(deg·g) (Privalov, 1979), and for the few coiled-coil proteins (e.g., tropomyosin, paramyosin, and light meromyosin) which have been studied, the values range from about 0.06 to 0.1 cal/(deg·g) (Privalov, 1982). The increase in heat capacity which occurs on protein unfolding has been attributed to the creation of ordered water in the vicinity of the exposed hydrophobic groups (Kauzman, 1959). We should point out that the determination of the  $\Delta C_p$  for unfolding using a single DSC scan, as we have done here, is susceptible to error due to imperfections in the base line before and after the transition. The presence of a broad endothermic transition on the high-temperature side of a DSC peak cannot be easily distinguished from a positive  $\Delta C_p$ . Curvature in the base line before or after the transition can make it difficult to decide how to fit or extrapolate the base line. Further studies will be required to determine  $\Delta C_p$  by studying the temperature dependence on  $\Delta H$ . Swenson and Ritchie (1980) determined a  $\Delta C_p$  for S-2 unfolding in this manner of 0.17 cal/(deg·g).

A comparison of the  $\Delta H_{\text{cal}}$  and  $\Delta H_{\text{vh}}$  values obtained for the globular head in HMM and S-1 indicates the presence of domains; however, the number of domains and their sizes are not indicated. We have attempted to unfold only some domains in the head by rapidly scanning to the midpoint of the transition and quickly cooling. Upon rescanning the sample, no endothermic transition was noted. In addition, we had expected that the binding of nucleotides to the active site might have preferentially stabilized part of the S-1. However, even in the presence of nucleotides which led to significant stabilization, only one peak was observed for the globular head in the DSC scan. Treatment of chymotryptic S-1 with trypsin had no effect on the thermodynamics of unfolding. We are thus led to the conclusion that domains in the head most likely exist, but they have nearly identical stabilities and they interact significantly.

Treatment of S-1 with trypsin results in the nicking of the myosin heavy chain which can be seen by the formation of three fragments on SDS gels of masses 20, 27, and 50 kDa. Some data have been presented which, it is argued, suggest that the 50-kDa "segment" of the myosin head is much more labile to thermal denaturation than the 27- and 20-kDa seg-

ments (Setton & Muhrad, 1984; Burke et al., 1987). In light of the data presented here, we would argue that the proteolysis experiments must be interpreted with caution. The addition of proteases during or following heat treatment can be expected to accelerate the unfolding of the protein in protease-sensitive regions, which will lead to further proteolysis. Thus, the absence of the 50-kDa fragment on SDS gels following heat treatment and trypsinization of S-1 does not indicate a cooperative, *global unfolding* of a 50-kDa domain, but rather an increased susceptibility to proteolysis by some portion of the 50-kDa segment. This is supported by the recent experiments of Cheung and Reisler (1988).

It might be suggested that the irreversible unfolding that occurs during prolonged (3 h) heat treatment of S-1 at 35 °C (Burke et al., 1987; Cheung & Reisler, 1988) could represent a small, local structural change in the 50-kDa segment which would not be observable by DSC. However, it should be noted that DSC scans are relatively rapid, e.g., 1.5 °C/min in this work. While it is not clear what state the S-1 is in after 3 h at 35 °C, it is certainly an unusual preparation, and it is not the same molecule that is being observed in the DSC at 35 °C (or possibly at any point during the scan). The irreversible transitions which have occurred after 3 h at 35 °C are ones that would normally have occurred at higher temperature in the DSC scan (as indicated by the requirement for a 3-h incubation time).

The shape of the S-1 denaturation endotherm, particularly in the presence of AMPPNP, is not symmetric, and it might be tempting to perform a deconvolution of the data to define a low-temperature transition. However, the gradual increase in excess heat capacity on the low-temperature side of the DSC peak is not indicative of a cooperative transition. We attribute the shape of the endotherm to the irreversibility of the reaction. As the temperature is increased and the endothermic peak is approached, heat will be absorbed by those molecules which unfold. In a reversible system, when the temperature is just below the region where the endothermic peak becomes obvious (e.g., 32 °C in Figure 5), most of the molecules which unfold will quickly refold, and the heat absorbed in the unfolding transition is returned to the system. Therefore, there is no net heat absorption. Only when the equilibrium constant deviates significantly from zero does the heat absorbed become significant since every molecule which unfolds does not necessarily refold. With an irreversible system, there is little refolding as the temperature is raised and molecules start to unfold. As a result, the net heat absorbed during the early part of the transition will be much greater than in a reversible system. Thus, DSC scans of irreversible transitions are expected to produce asymmetric endotherms.

#### ACKNOWLEDGMENTS

We thank Dr. Wayne Bolen, Dr. Marcello Santoro, and Dr. Julian Sturtevant for helpful discussions during this work.

#### REFERENCES

- Balint, M., Wolf, L., TarcsaFalvi, A., Gergeley, J., & Sreter, F. (1978) *Arch. Biochem. Biophys.* 190, 793–799.
- Burke, M., Zaagler, S., & Bliss, J. (1987) *Biochemistry* 26, 1492–1496.
- Chaussepied, P., Mornet, D., Audemard, E., Kassab, R., Goodearl, A., Levine, B., & Trayer, I. (1986) *Biochemistry* 25, 4540–4547.
- Cheung, P., & Reisler, E. (1988) *Arch. Biochem. Biophys.* 265, 272.
- Cross, R., Bardsley, R., Ledward, D., Small, J., & Sobieszek, A. (1984) *Eur. J. Biochem.* 145, 305–310.



- Goodno, C. (1979) *Proc. Natl. Acad. Sci. U.S.A.* 76, 2620-2624.
- Goodno, C., & Swenson, C. (1975) *Biochemistry* 14, 873-878.
- Gordon, A., & Ford, R. (1972) *The Chemist's Companion*, Wiley, New York.
- Griffiths, A., & Trayer, I. (1989) *FEBS Lett.* 242, 275.
- Harrington, W., & Ueno, H. (1987) *Biopolymers* 26, S81-S98.
- Hvidt, S., Rodgers, M., & Harrington, W. (1985) *Biopolymers* 24, 1647-1662.
- Hynes, T., Block, S., White, B., & Spudich, J. (1987) *Cell* 48, 953-963.
- Jacobson, A., & Henderson, J. (1973) *Can. J. Biochem.* 51, 71-86.
- Kamath, U., & Shriver, J. (1989) *J. Biol. Chem.* 264, 5586-5592.
- Kauzman, W. (1959) *Adv. Protein Chem.* 14, 1-63.
- Kay, L., Pascone, J., Sykes, B., & Shriver, J. (1987) *J. Biol. Chem.* 262, 1984-1988.
- King, L., & Lehrer, S. (1989) *Biochemistry* 28, 3498.
- Margossian, S., & Lowey, S. (1982) *Methods Enzymol.* 85, 55-71.
- Mornet, D., Pantel, P., Bertrand, R., Audemard, E., & Kassab, R. (1981) *FEBS Lett.* 123, 54-58.
- Mornet, D., Ue, K., & Morales, M. (1984) *Proc. Natl. Acad. Sci. U.S.A.* 81, 736-739.
- Muhlrad, A., & Morales, M. (1984) *Proc. Natl. Acad. Sci. U.S.A.* 81, 1003-1007.
- Okamoto, Y., & Sekine, T. (1987) *J. Biol. Chem.* 262, 7951-7954.
- Privalov, P. (1979) *Adv. Protein Chem.* 33, 167-241.
- Privalov, P. (1982) *Adv. Protein Chem.* 35, 1-104.
- Privalov, P., Griko, Y., Venyaminov, S., & Kutysenko, V. (1986) *J. Mol. Biol.* 190, 487-498.
- Setton, A., & Muhlrad, A. (1984) *Arch. Biochem. Biophys.* 235, 411-417.
- Shriver, J., & Sykes, B. (1981) *Biochemistry* 20, 2004-2012.
- Sturtevant, J. (1987) *Annu. Rev. Phys. Chem.* 38, 463-488.
- Sutoh, K., Sutoh, K., Karr, T., & Harrington, W. (1978) *J. Mol. Biol.* 126, 1-22.
- Swenson, C., & Ritchie, P. (1980) *Biochemistry* 19, 5371-5375.
- Takahashi, K., Casey, J., & Sturtevant, J. (1981) *Biochemistry* 20, 4693-4697.
- Ueno, H., Rodgers, M., & Harrington, W. (1983) *J. Mol. Biol.* 168, 207-228.
- Vibert, P., & Cohen, C. (1988) *J. Muscle Res. Cell Motil.* 9, 296-305.
- Wagner, P. (1984) *Biochemistry* 23, 5950-5956.
- Weeds, A., & Taylor, R. (1975) *Nature* 257, 54-56.
- Weeds, A., & Pope, B. (1977) *J. Mol. Biol.* 111, 129-157.
- Zehfus, M. (1987) *Proteins: Struct., Funct., Genet.* 3, 90-110.

## pH Dependence of the Urea and Guanidine Hydrochloride Denaturation of Ribonuclease A and Ribonuclease T1<sup>†</sup>

C. Nick Pace,\* Douglas V. Laurents, and James A. Thomson

Biochemistry Department, Texas A&M University, College Station, Texas 77843

Received September 5, 1989; Revised Manuscript Received November 6, 1989

**ABSTRACT:** To investigate the pH dependence of the conformational stability of ribonucleases A and T1, urea and guanidine hydrochloride denaturation curves have been determined over the pH range 2-10. The maximum conformational stability of both proteins is about 9 kcal/mol and occurs near pH 4.5 for ribonuclease T1 and between pH 7 and 9 for ribonuclease A. The pH dependence suggests that electrostatic interactions among the charged groups make a relatively small contribution to the conformational stability of these proteins. The dependence of  $\Delta G$  on urea concentration increases from about 1200 cal mol<sup>-1</sup> M<sup>-1</sup> at high pH to about 2400 cal mol<sup>-1</sup> M<sup>-1</sup> at low pH for ribonuclease A. This suggests that the unfolded conformations of RNase A become more accessible to urea as the net charge on the molecule increases. For RNase T1, the dependence of  $\Delta G$  on urea concentration is minimal near pH 6 and increases at both higher and lower pH. An analysis of information of this type for several proteins in terms of a model developed by Tanford [Tanford, C. (1964) *J. Am. Chem. Soc.* 86, 2050-2059] suggests that the unfolded states of proteins in urea and GdnHCl solutions may differ significantly in the extent of their interaction with denaturants. Thus, the conformations assumed by unfolded proteins may depend to at least some extent on the amino acid sequence of the protein.

**R**ibonuclease A (RNase A) from bovine pancreas is one of the most thoroughly studied enzymes, and the energetics (Hermans & Scheraga, 1961; Schwarz & Kirchhoff, 1988) and mechanism (White & Anfinsen, 1959; Wearne &

Creighton, 1988; Udgaonkar & Baldwin, 1989) of folding have been studied in detail over the past 30 years. Ribonuclease T1 (RNase T1) from *Aspergillus oryzae* is the next best characterized ribonuclease and has proven to be an excellent model for investigating several aspects of protein folding (Thomson et al., 1989; Shirley et al., 1989; Pace & Laurents, 1989). These enzymes share a function, but they do not resemble one another in amino acid sequence or three-di-

<sup>†</sup>Supported by grants from the NIH (GM 37039), the Robert A. Welch Foundation (A 1060), and the Texas Agricultural Experiment Station.